

# Progress in ocean wave forecasting at ECMWF

Peter Janssen, Jean-Raymond Bidlot,  
Saleh Abdalla and Hans Hersbach

Research Department

September 2005

*This paper has not been published and should be regarded as an Internal Report from ECMWF.  
Permission to quote from it should be obtained from the ECMWF.*



European Centre for Medium-Range Weather Forecasts  
Europäisches Zentrum für mittelfristige Wettervorhersage  
Centre européen pour les prévisions météorologiques à moyen terme

Series: ECMWF Technical Memoranda

A full list of ECMWF Publications can be found on our web site under:

<http://www.ecmwf.int/publications/>

Contact: [library@ecmwf.int](mailto:library@ecmwf.int)

©Copyright 2005

European Centre for Medium-Range Weather Forecasts  
Shinfield Park, Reading, RG2 9AX, England

Literary and scientific copyrights belong to ECMWF and are reserved in all countries. This publication is not to be reprinted or translated in whole or in part without the written permission of the Director. Appropriate non-commercial use will normally be granted under the condition that reference is made to ECMWF.

The information within this publication is given in good faith and considered to be true, but ECMWF accepts no liability for error, omission and for loss or damage arising from its use.

## Abstract

In the 1980's the introduction of the first supercomputers and the promise of the wealth of data on the ocean surface from remote-sensing instruments on board of new satellites such as ERS-1 and Topex-Poseidon provided a significant stimulus to the development of a new generation of ocean wave prediction models. The Wave Model (WAM) group emerged and the main goal was to develop a spectral ocean wave model based on solving the energy balance equation which included explicitly the physics of wind-wave generation, dissipation due to white capping and nonlinear interactions. Development of this new wave prediction system was rapid and ECMWF helped by providing resources (in terms of computing facilities, advice by staff and office space). In July 1992 the WAM model became operational at ECMWF.

Based on the experience of wave modellers such as the people from the WAM group it was clear at that time that the quality of wave forecast results was to a large extent determined by errors in the forcing wind field. Since the winds gave such a large contribution to the error budget of, for example, the significant wave height, it was expected that it would be difficult to improve the wave model.

In this topic paper we discuss progress in ocean wave forecasting during the past 10 years. It will be shown that during this period there have been substantial improvements in the quality of the forecast surface wind field and as a consequence also in the quality of the forecast wave height field. This follows from comparisons with the verifying analysis, in-situ buoy data and altimeter data. The reasons for these large improvements are detailed in the paper; the improvements mainly come from the introduction of 4DVAR, increases in atmospheric resolution, improvements of the physics of the atmospheric model and the two-way interaction of wind and waves.

Because of the large error reduction in the forcing winds, it is nowadays easier to improve the wave model. Examples of recent wave model improvements are the introduction of wind gustiness, the introduction of the effects of unresolved bathymetry and the revised formulation of wave dissipation. These recent changes have not only resulted in a closer fit to the observations but have also given a larger, more realistic variability in modelled wave height and mean frequency.

Finally, we also briefly discuss a number of new developments. An important element of severe weather forecasting over the oceans is the prediction of freak waves. Here, we describe the steps that led to the introduction of the first operational freak wave prediction system. The sea state is affected by ocean currents, tides and storm surges. Here, we discuss first results regarding the impact of ocean currents on the significant wave height field on a global scale. It is argued that for sea state forecasting in the coastal zone, an area of important economic significance, knowledge of the (ocean) current and the mean sea level is important. Therefore, a proper modelling of the sea state in the coastal zone will require the introduction of a coupled storm-surge, ocean wave prediction system.

## 1 Introduction

In this topic paper a brief overview of the ECMWF wave forecasting system is given. The present applications of the wave forecasting model are described, followed by a discussion of some developments of the wave model after the operational introduction of WAM cy4 in 1992. In particular, the main reason is given why the present version of the atmospheric model with spatial resolution of 40 km and 60 layers in the vertical shows a sensitive dependence on the two-way interaction between wind and waves. Extensive validation of wave analysis and forecast is performed at ECMWF. For example, analysed/ first-guess wave height verification against buoy data and altimeter data is discussed, while verification of the 10-day forecasts against the analysis is given as well. Conclusive evidence is found of the sensitive dependence of wave forecasting results on the quality of the surface wind field. Since independent validation of the surface winds suggests that in the past five years there have been considerable improvements in the quality of the surface wind field on a global scale, the time is ripe to reconsider numerics and physics of the wave prediction model. As a first step, results with a revised formulation of the dissipation source function are presented. Also, work on a revised version of the nonlinear

transfer is discussed.

The last few years there has been a rapid increase in our understanding of the formation of extreme sea states, usually called freak waves. In the early 1960's there was a rapid development of the statistical theory of ocean waves, culminating in the basic evolution equation for the ocean wave spectrum: the **energy balance equation**. To lowest order, the probability distribution function (pdf) for the surface elevation was found to be a Gaussian, corresponding to linear waves. It was not realized at that time, however, that effects of finite amplitude on the pdf can be calculated and result in valuable information on extreme sea states. A simplified version of the calculation of the pdf was introduced in operations recently.

## 2 WAM cy4 and operational applications

The present version of the ECMWF wave forecasting system is based on WAM cy4 as described by Komen *et al* (1994). The WAM model is the first model that explicitly solves the energy balance equation. The usual wave number spectrum is denoted by  $F(\vec{k}; \vec{x}, t)$ . In wave dynamics the fundamental quantity to predict is, however, the action density spectrum  $N(\vec{k}; \vec{x}, t)$ . It is defined as

$$N = \frac{gF}{\sigma} \quad (1)$$

with  $\sigma = \sqrt{gk \tanh(kD)}$ . The action density plays the role of a number density of waves, hence (apart from the constant water density) the energy  $E$  of the waves is given by  $E = \sigma N$ , while the wave momentum  $\vec{P}$  is given by  $\vec{P} = \vec{k}N$ .

The energy balance equation follows from Whitham's variational approach in a straightforward manner (Janssen, 2004) and the result for waves on a slowly varying current  $\vec{U}$  is

$$\frac{\partial N}{\partial t} + \nabla_{\vec{x}} \cdot (\nabla_{\vec{k}} \Omega N) - \nabla_{\vec{k}} \cdot (\nabla_{\vec{x}} \Omega N) = S. \quad (2)$$

Here,  $\Omega$  represents the dispersion relation

$$\Omega = \vec{k} \cdot \vec{U} + \sigma, \quad (3)$$

The source function  $S$  on the right hand side of Eq. (2) represents the physics of wind-wave generation ( $S_{in}$ ), dissipation by wave breaking and other causes ( $S_{dissip}$ ) and four-wave interactions ( $S_{nonlin}$ ). In other words,

$$S = S_{in} + S_{nonlin} + S_{dissip}. \quad (4)$$

In the 1980's there was a major effort to develop realistic parametrisations of all the source functions. The present version of the WAM model has an input source function which is based on Miles critical layer mechanism (Miles, 1957) (including the feedback of the wave stress on the wind profile (Janssen, 1989)), the nonlinear interactions are represented by means of the direct-interaction approximation (DIA) of Hasselmann *et al* (1985) while the dissipation source function is based on the work of Hasselmann (1974). A first account of this is given by Komen *et al* (1994), while a more up to date account of the status of wave modelling, including most of the new developments discussed in this paper, can be found in Janssen (2004).

The WAM model was introduced in operations in June 1992. Since that date there has been a continuous programming effort to keep the software up to date. For example, in order to improve efficiency, options for macrotasking (later replaced by open MP directives) and massive parallel processing were introduced. In addition, the software now fully complies with Fortran 90 standards. The advantage of this is that only one

executable is needed for all the relevant applications, such as the deterministic forecast with resolution of 55 km, the ensemble forecast with resolution of 1 degree and the limited area forecasts with a resolution of 28 km. The same executable can also be run as a one grid point model, which is convenient when testing changes in physics for example. Finally, over the past 10 years a number of model changes were introduced which will be discussed in some detail in Section 3. A documentation of the present version of the ECMWF wave model may be found on the web(<http://www.ecmwf.int/>; click research, click on 'Full Scientific and technical documentation of the IFS' and finally choose Chapter VII).

Presently the wave model is run for the global domain and as a limited area model for the waters surrounding Europe. This note will concentrate on the global domain. The global model covers an area of 81 deg S to 81 deg N. Since the 29th of June 1998 the wave model is part of the IFS model enabling a two-way interaction between wind and waves. Hence, the sea surface roughness, as seen by the atmosphere, is sea state dependent.

For the globe two medium-range applications are run:

- **Deterministic Forecast.** The resolution of the wave model is 55 km. The spectrum consists of 30 frequencies and 24 directions, and shallow water effects are switched on. In order to avoid violation of the CFL criterion in the polar regions an irregular lat-lon grid was introduced in such a way that in the latitude direction the distance between grid points is more or less constant. This has the additional benefit that compared to normal spherical coordinates the number of grid points reduces by 30%. The integration and propagation time step are 15 minutes. The wave model is coupled to the 10 m neutral winds of the  $T_1511$  atmospheric model and the coupling time step is 15 minutes. Benefits of two-way interaction are reviewed in Janssen *et al*(2002) and Janssen (2004). In the analysis step altimeter wave height data are assimilated using the OI scheme of Lionello *et al* (1992) while Synthetic Aperture Radar (SAR) spectra are assimilated as well. In order to assimilate the spectral information a partition method is used distinguishing between wind sea and a number of swell components. The OI scheme of Lionello *et al* is then applied to each partitioning. Every day 10 day forecasts are issued from 12Z and 00Z.
- **Probabilistic Forecasts.** ECMWF produces ensemble weather forecasts since December 1992. With the introduction of two-way interaction of wind and waves it was relatively straightforward to introduce ensemble forecasting of ocean waves. An ensemble of forecasts is realised by perturbing the atmospheric initial state with a set of the most unstable singular vectors, while the initial sea state is not perturbed. Presently, everyday 50 ensemble members and one control forecast are produced. The resolution of the wave model is 110 km and it is coupled to the 10 m winds of the  $T_1255$  atmospheric model.

Ensemble wave products are helpful in assessing the uncertainty in the wave forecast, in estimating probabilities of high sea states in the medium-range and in practical applications such as ship routing (Hoffschildt *et al*, 1999) An extensive validation of the EPS wave forecast may be found in Saetra and Bidlot (2004) and in Saetra *et al* (2004).

The wave model software is furthermore run for the boundary conditions suite, monthly forecasting, seasonal forecasting and for the reanalysis.

### 3 Developments after WAM cy4

Apart from the extensive code developments in order to be able to run the WAM model software on multi processor machines, changes to the WAM software have been introduced as well. In the first instance these have been mainly of a numerical nature, i.e. there were no changes to the formulation of the physical processes, only to its numerical representation.

Recently, warranted by the considerable improvements in the model surface winds, a number of changes to the physics of the model have been introduced as well. These concern the introduction of the effects of gustiness and a revised formulation of wave dissipation.

The major changes that have been introduced are listed in the following subsections

### 3.1 Advection scheme

In order to alleviate problems with wave energy propagation along the coordinate axes the spectrum was rotated by 1/2 its angular resolution. This change was introduced in May 1997. As discussed by Bidlot *et al* (1997), this change resulted in occasionally large improvements in the shadow zones of islands such as Hawaii. Overall, it gave a small improvement on the scores of large areas such as the Tropics.

### 3.2 Integration scheme

Physical processes such as wind-wave generation, nonlinear transfer and wave dissipation occur, in particular for the high-frequency waves, on a short time scale. For this reason, the wave model employs an implicit scheme, which involves the functional derivative of the source function  $S$  with respect to the wave spectrum (giving a two-dimensional matrix). The functional derivative matrix needs to be determined and needs to be inverted, which is very cumbersome. Therefore, only the diagonal elements of the matrix are determined so that the inversion is straightforward, but there is no guarantee that the numerical scheme is stable. For this reason a wave growth limiter is needed as well. Unfortunately, the original limiter was not dimensionally correct and in some cases too restrictive.

A more liberal, dimensionally correct limiter of wave growth was introduced following the work of Hersbach and Janssen (1999). This change is particularly relevant in fetch-limited, rapidly varying circumstances. Also, originally the time-integration scheme was semi-implicit, but Hersbach and Janssen found that a fully implicit scheme gave a favourable noise reduction (Change introduced in December 1996).

Furthermore, for coupling purposes the Charnock parameter needs to be evaluated. In the original version of WAM this parameter was determined before the wave spectrum was updated, hence there is a mismatch of one time step between sea state and roughness length. In the present versions (since CY 24R2, January 2002) the Charnock parameter is also determined after the spectral update, thus avoiding the mismatch in time. This change resulted in considerable improvements in forecasting of weather parameters, avoiding the generation of spurious lows in the  $T_1$  511 version of the IFS (see Fig. 1). Also a beneficial impact on atmospheric scores was noted, in particular in the Southern Hemisphere.

### 3.3 Two-way interaction of wind and waves

This major change was introduced in operations in June 1998. At the same time this facilitated the operational running of ensemble wave forecasts.

A review of the impact of two-way interaction on the atmosphere is given in Janssen *et al* (2002). At the time of operational introduction of the coupling there was an evident reduction of the systematic error in forecast wave height (verified against analysis) and the standard deviation of error was reduced by about 5%. Also, as illustrated in Fig. 2, the rms error in first-guess wind speed verified against scatterometer winds was reduced by 10%. There was also some impact on the accuracy of forecast atmospheric parameters, e.g. the 1000 and 500 mb geopotential in the Southern Hemisphere. The main point of the review is, however, that the impact of

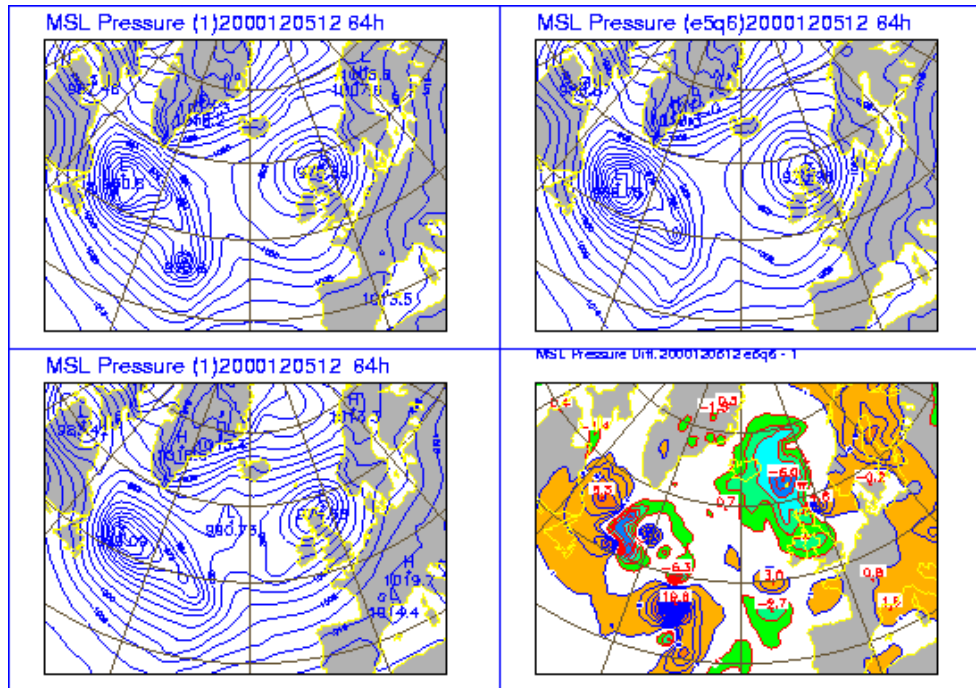


Figure 1: Impact of the revised roughness length determination on removing a rapidly developing system in the short-range. The left top panel is control forecast, the right top panel is the forecast with the new scheme, the left bottom panel is the verifying analysis and the right bottom panel is the difference between experiment and control.

sea state dependent drag on the atmospheric flow has increased over the years simply because the resolution of the atmospheric model has increased. This increase in resolution has resulted in a more realistic representation of the sub-synoptic scales, which are the ones that are relevant for the interaction of wind and waves. The point is perhaps best illustrated by the operational introduction of the  $T_1$  511 atmospheric system. At the same time it was decided to increase directional resolution of the wave spectrum by a factor of two from 12 to 24 directions while also a more accurate determination of the energy fluxes in the advection scheme was introduced. In the context of the lower resolution  $T_1$  319 atmospheric model it was possible to show that the proposed wave model changes had a small but positive impact on atmospheric and wave scores. However, in the context of  $T_1$  511 impact was much more pronounced, as discussed in more detail in Janssen *et al* (2002). The main reason for this is probably that in  $T_1$  511 the subsynoptic scales are better represented, which follows by comparing for  $T_1$  511 and  $T_1$  319 plots of the Kinetic Energy spectrum near the surface as function of total wave number.

### 3.4 Dynamic range

The wave model physics is only valid in a limited frequency range, typically below 2.5-3 times the peak frequency of windsea. For higher frequencies micro-scale breaking becomes an important process giving an  $\omega^{-5}$  spectrum, but we cannot model this process explicitly. For this reason, the spectrum is determined up to a certain cut-off frequency, while for higher frequencies Phillips'  $\omega^{-5}$  spectrum is assumed where the energy level is determined by the spectrum at the cut-off.

In WAM cy4 the cut-off frequency  $f_c$  was

$$f_c = \max(2.5f_{mean}, 4f_{PM}) \quad (5)$$

with  $f_{PM}$  the so-called Pierson Moskowitz frequency ( $f_{PM} = 0.00568g/u_*$ , with  $u_*$  the friction velocity) and

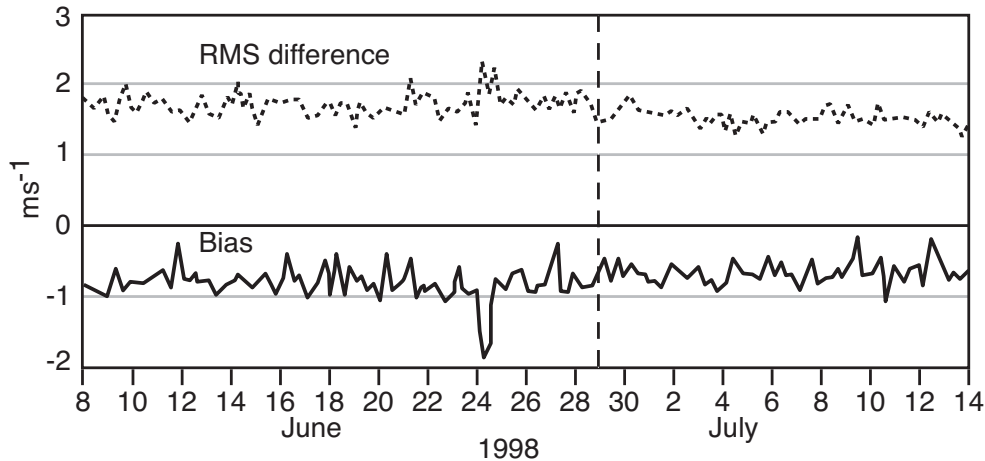


Figure 2: Bias (ERS-2 minus EC FG) and rms difference between the background ECMWF surface winds and the ERS-2 scatterometer wind measurements. The vertical dashed line shows the date when two-way interaction was introduced operationally.

$f_{mean}$  is a suitably defined mean frequency.

The new choice is simply  $f_c = 2.5f_{mean}$ . This change resulted in a more realistic dependence of the rms slope and the Charnock parameter on the surface wind speed, while first-guess wave height standard deviation errors, as compared to altimeter wave height data, were reduced by 5% (cf Janssen *et al*, 2002). This change was introduced in July 1999. It was not realized at that time that there also was a detrimental impact. The new choice of cut-off frequency is too restrictive so that in low wind speed areas and in the presence of low-frequency swell (as occurs e.g. in the Tropics) windseas cannot be generated. This has probably resulted in too low a variability in the Tropical wave heights (see for an example Kumar *et al* (2003)), giving an undesirable artificial improvement of the Tropical scores for wave height.

### 3.5 Altimeter data and normality

Altimeter wave height observations are important for the wave analysis and for validation of the wave forecast. An altimeter is a nadir looking Radar and the Radar return signal (called the 'wave form') is caused by specular reflection from the crests and the troughs of the ocean waves. Hence the wave form is determined by the joint probability distribution function of surface elevation and slope. Altimeter wave heights are obtained from the wave form by assuming that the sea state is Gaussian. However, owing to nonlinearity, deviations from the Gaussian state occur. These deviations from Normality can be obtained using the wave spectrum. Applying the thus obtained correction one finds in coastal areas that this may give an increase in wave height of 10%, although over all cases the correction is only 3% (Janssen, 2000). This correction to altimeter wave heights was introduced in July 1999, while also the corresponding corrections to the altimeter range measurements were introduced and archived.

### 3.6 Wind forcing

Following the work of Abdalla and Cavaleri (2002) effects of wind gustiness and variable air density on the input source function was introduced in April 2002. Here, the gustiness level is obtained from an empirical formulation by Panofsky *et al* (1977), while the mean impact of gustiness on the wind input is approximated by

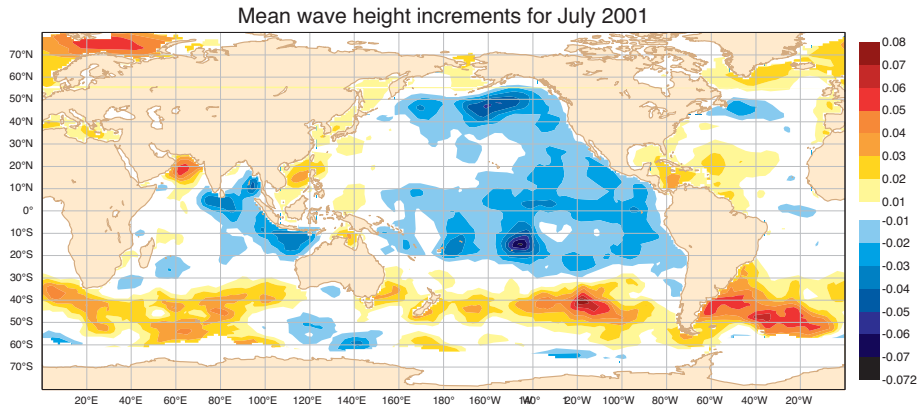


Figure 3: Mean wave height analysis increments for July 2001 (in meters). ERS-2 altimeter data were the only data used in the data assimilation. The stand alone WAM on a 55 km grid was used.

means of Gauss-Hermite quadrature (following a suggestion by John Miles). These changes had a beneficial impact on wave height scores for Tropics and the Southern Hemisphere.

Until March 2004 the wave model was forced by surface winds. Ideally, one would like to force with surface stresses. Because of inconsistencies between surface winds and stress (Janssen *et al*, 1992), early experiments in the mid 1980’s showed very disappointing results, as extreme events were underestimated rather seriously. Therefore, from early on wave models have been driven by surface winds. However, the inconsistency between surface stress and surface winds had already been resolved with the  $T_1$  213 version of the atmospheric model by removing a time step dependency in the wind speed determination (Janssen *et al* 1992). It was therefore clearly time to try forcing with surface stresses once more. Forecast results showed a positive impact of using stresses, in particular in regions where stability effects (e.g. the Gulf Stream) play a role. This change was introduced in operations in March 2004.

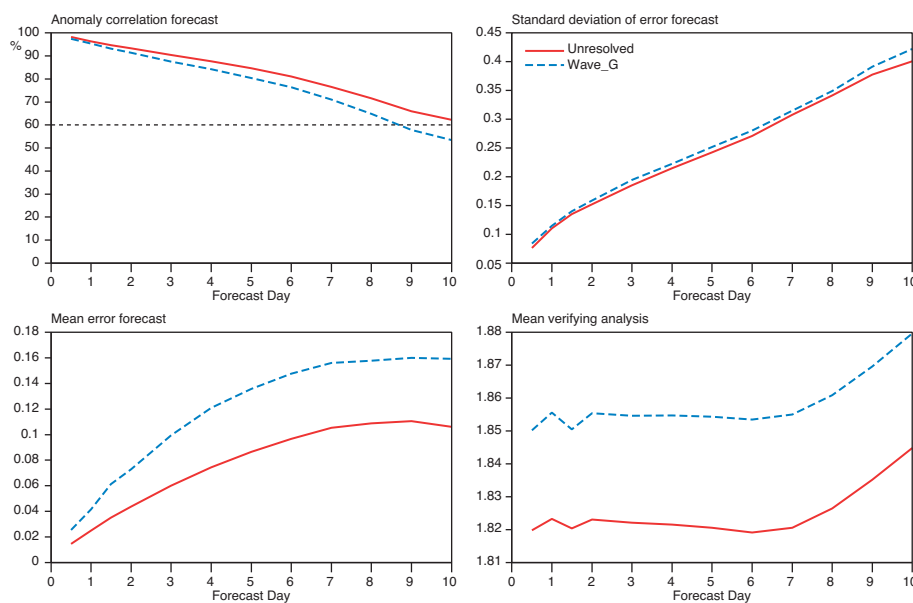


Figure 4: Wave height scores against own analysis for the Tropical area. The reference is operations.

### 3.7 Unresolved bathymetry

Inspecting maps of monthly mean analysis wave height increments, especially during the Northern Hemisphere summer (Fig. 3), it appears that there are areas where the wave model first guess is systematically too high or too low. The underestimation in wave heights tends to be located in the active storm track areas or in areas affected by the Indian sub-continent monsoon. This underestimation is likely caused by too weak model winds. On the other hand, the overestimation for most of the tropical and northern Pacific cannot be explained in terms of local winds. After further scrutiny, it appears that these systematic overestimations are often present in areas where small island chains exist (French Polynesia and Micronesia in the Pacific Ocean, Maldives Islands and Andaman Islands in the Indian Ocean and Azores and Cape Verde Islands in the Atlantic Ocean).

These small scale features are not well-resolved by the present operational grid which has a resolution of 55 km, and it would be far too expensive to resolve these features explicitly. Nevertheless, small island can block considerable amounts of wave energy. In order to represent these unresolved features we have introduced in the wave model's advection scheme a wave number dependent blocking factor. Here the blocking factor was determined by estimating from the high resolution ETOPO2 topographic data set how much energy the unresolved features will block. This change resulted in a large impact on the Tropical wave height scores, in particular the anomaly correlation (Fig 4). The effects of unresolved bathymetry were introduced in March 2004.

### 3.8 Dissipation

The dissipation source function is probably the least well-known source function in ocean wave modelling. In the past it has been determined starting from the assumption that wind input and nonlinear transfer are well-established and the dissipation term is then determined in such a way that in the steady state the observed Pierson-Moskowitz spectrum is reproduced (Komen *et al*, 1984). In this tuning exercise the dissipation source function is given by the general form

$$S_{ds} = -\gamma_d N, \tag{6}$$

with

$$\gamma_d = \beta \langle \omega \rangle \langle \langle k \rangle^2 m_0 \rangle^m \left[ (1 - \alpha) \frac{k}{\langle k \rangle} + \alpha \left( \frac{k}{\langle k \rangle} \right)^2 \right]. \tag{7}$$

Here,  $\beta$ ,  $\alpha$  and  $m$  are constants which need to be determined, while mean frequency  $\langle \omega \rangle$  and wavenumber  $\langle k \rangle$  are defined in a suitable manner. The parameter  $\langle \langle k \rangle^2 m_0 \rangle$  is an integral measure for the square of the wave steepness, thus, in agreement with one's intuition the dissipation increases for increasing steepness.

In the mid 1980's it was first suggested to base the mean frequency on the first moment of the spectrum,

$$\langle \omega \rangle = \int d\vec{k} \omega F(\vec{k}) / \int d\vec{k} F(\vec{k}) \tag{8}$$

with a similar relation for the mean wavenumber. However, initial experiments showed fairly noisy results and the definition in terms of the first moment was abandoned in favour of one in terms of the inverse mean frequency, or

$$\langle \omega \rangle = \int d\vec{k} F(\vec{k}) / \int d\vec{k} F(\vec{k}) / \omega. \tag{9}$$

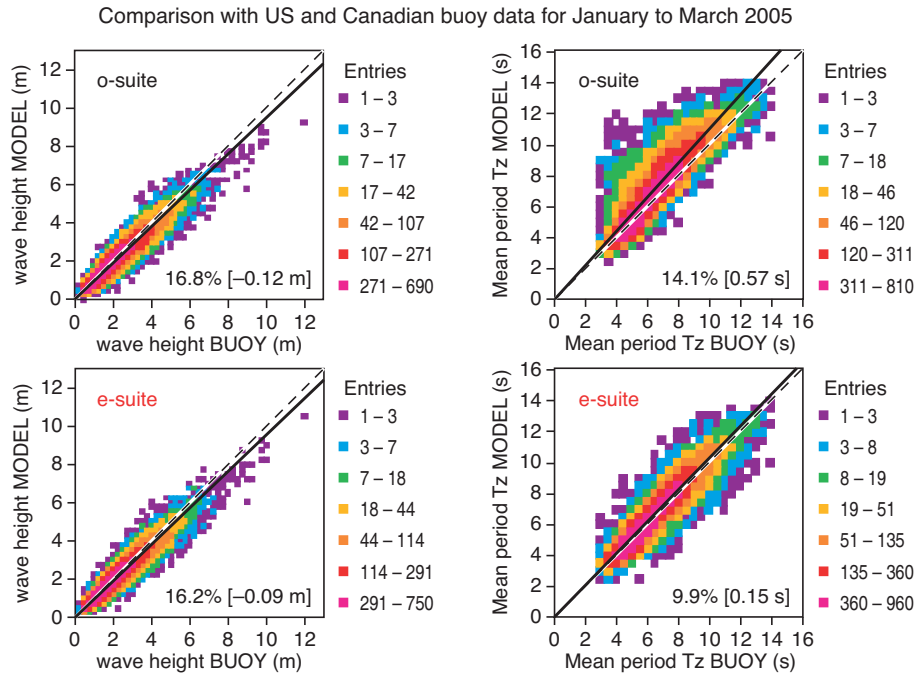


Figure 5: Comparison of wave height and mean Period scores against buoy observations from o and e-suite for the three month period of January to March 2005.

And indeed, because the latter definition gives more emphasis on the slowly-varying low-frequency part of the spectrum, results are much less noisy, and the definition (9) for mean frequency has been used ever since.

A drawback of the use of the inverse mean frequency was only just recently realized. In the presence of low-frequency swell the dissipation of windsea turns out to be largely determined by the swell part of the spectrum. In fact, because the steepness of swell is usually small, the dissipation of windsea in the presence of swell is much smaller than in its absence. As a consequence, windseas have more energy in the presence of swell, which contrasts common knowledge and belief.

It was decided to return to the use of the mean parameter definition (8) as this does not suffer from the above mentioned drawback. In addition, as now in the presence of swell the dissipation of windsea is much larger we could relax the definition of the dynamic integration range given in Section 3.4 so that windseas are properly generated, also in the Tropics. Thus, the dynamic range is now defined by all frequencies below the cut-off frequency  $f_c$ , with

$$f_c = 2.5 f_{mean,ws} \quad (10)$$

where  $f_{mean,ws}$  is the mean frequency of the windsea.

The combination of these two changes gave a considerable impact on the analysis of parameters such as the mean frequency as shown in Fig. 5, which gives a comparison of scores of o-suite and e-suite against buoy observations over a three month period. A reduction in random error of 30% is an example of a large improvement. Note that this is not even the most extreme example of improvement: from around the Indian continent we recently started receiving buoy data. Against these data the e-suite showed a reduction in the error of the mean frequency by a factor of two.

It is emphasized that these considerable improvements in spectral shape are caused by the introduction of a much wider dynamical range, made possible by the revised formulation of the dissipation source function. This allows the proper treatment of windsea in the presence of low-frequency swell. The consequence is, however,

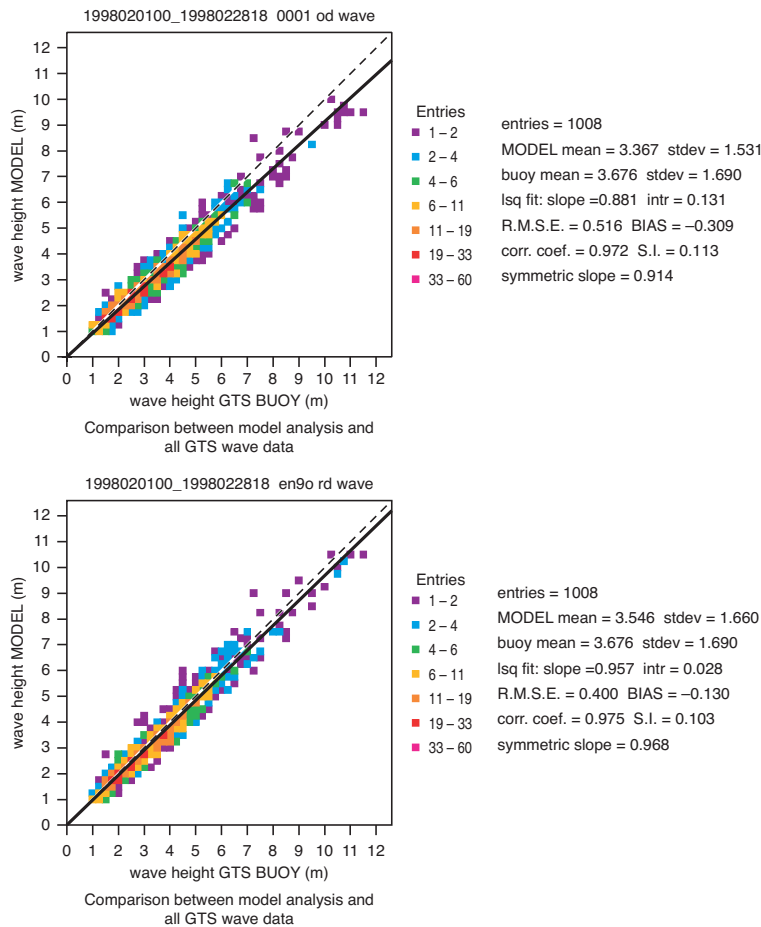


Figure 6: Comparison of analyzed wave height errors against buoy data around the UK of CY 29R1 (bottom) and operations (WAM4r7) (top) for February 1998.

that variability in wave height has increased, in particular in the Tropics. Also, since the dissipation source function is now determined in terms of the first moment of the spectrum, wave model results have become more sensitive to details in the high-frequency part of the spectrum. As the short waves are determined to a large extent by the wind, wave model results have become more sensitive to changes in the wind, in particular more sensitive to errors in the wind forcing. Therefore, when comparing wave forecasts against the own analysis wave height scores of the e-suite were in the medium range slightly worse compared to the o-suite. However, scoring the forecast results against ENVISAT altimeter data showed a small improvement in wave height scores, in particular in the Southern Hemisphere. The change was introduced in operations in April 2005.

### 3.9 'Overall' impact

It is of interest to have an idea whether these wave model changes combined have, for given wind forcing, resulted in an improved specification of the sea state. Therefore, the standalone version of Cycle 29R1 was rerun for the month of February 1998 using operational analysed winds, and wave height scores against buoy data were compared with the ones produced by the operational wave model at that time. Note that the operational model of February 1998 already included the changes mentioned in Sections 3.1 and 3.2, while obviously with a standalone run we do not test the possible improvements brought by the two-way interaction of wind and waves. Therefore, only the impact of the changes mentioned in section 3.4, 3.6, and 3.7 are tested here. Overall,

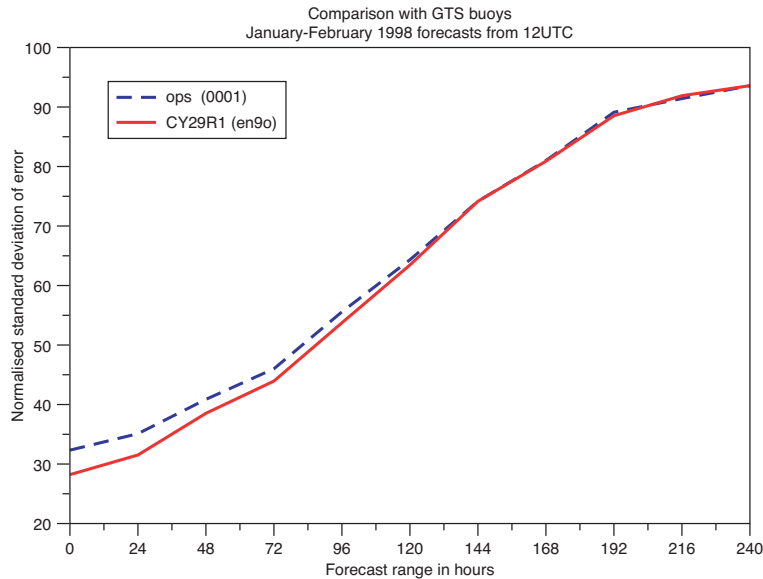


Figure 7: Normalised standard deviation of forecast wave height error for operations and Cy 29R1 for the two month period of January and February 1998. The models have been forced by the same, analysed surface wind speeds.

it turns out that these changes have reduced the rms error of analysed wave height by 15%, reducing the rms error against buoy data from 0.59 to 0.50 m. Variability has increased by about 7% and is in good agreement with observed variability. An example of a comparison plot is given in Fig. 6 and shows statistics for all buoys around the U.K. Note that the increase in the symmetric slope corresponds directly to the increased variability.

The increase in variability by the CY 29R1 version of the wave forecasting system leads, as can be easily verified by means of a simple analysis, to larger rms errors in the medium to long-range. In order not to be penalized by the increased, more realistic variability, we show in Fig. 7 the normalised standard deviation of forecast wave height error (*nsd*) as function of forecast time for both the operational results and CY 29R1. Here, the *nsd* is obtained by normalising the standard deviation of error by means of the variance in observed and model wave height. In terms of this score it is seen that CY 29R1 is outperforming the 1998 operational wave model up to 5 days in the forecast. Beyond that range the wind speed error is so large that it probably dominates the forecast wave height error (see next Section).

## 4 Verification and sensitive dependence on wind speed error

At ECMWF there is an extensive effort to validate analysis against available, independent buoy data, while the forecast is compared with buoy data, altimeter wave height data and the verifying analysis. For an overview of the quality of the ECMWF wave forecasting system in 1995 see Janssen *et al* (1997). For the period between 1995 and 2003 see Janssen (2004), while an up-to-date version of the verification results is given in Appendix A.

In addition, regarding the validation of analysis and forecast against buoy data, ECMWF is involved in an intercomparison project with centres such as UKMO, FNMOC, CMS, NCEP, Météo-France and DWD. In comparison with other centres, the ECMWF wave forecasting system shows a relatively slow deterioration of the forecast. A more detailed discussion of this may be found in Bidlot *et al* (2002) and for up-to-date results see the Appendix.

As reported by Janssen *et al* (2000) and in the Appendix, we have seen a steady improvement in forecast skill of waveheight. From the comparison of forecast surface winds and wave heights with the verifying analysis it turns out that over the last 10 years the standard deviation of error in wind speed and wave height has been reduced by 40% in the Northern Hemisphere, while improvements in the Southern hemisphere are similar. Also, when comparing first-guess wave height and analysed wind speed with the counterparts measured by the ERS-2 altimeter (Janssen, 2004), considerable reductions in the standard deviation of error are found. For example, first-guess wave height error is reduced from about 50-60 cm in 1994 to around 30 cm presently, while the analysed wind speed error reduced from about 2 m/s to about 1.3 m/s.

It is believed that a considerable part of the improved skill in wave forecasts is caused by the improvements in surface winds. This follows from Janssen(1998) who established, based on the verification results of forecast wind and waves against the analysis, a close relation between the wave height error and the wind speed error. Up to the year 2000 the improvements in the quality of the surface winds were caused by the introduction of CY13R4 (which included a number of physics changes such as the introduction of a new subgrid orographic scheme and a return to mean orography), 3DVAR (including the use of Scatterometer data), the formulation of the new Jb, 4DVAR (which allowed a better treatment of Satellite data from e.g. (A)TOVS), the introduction of the  $T_l$  319 version of the IFS and the two-way interaction of wind and waves (Janssen *et al*, 2000). After that date we mention the introduction of the  $T_l$  511 version of the IFS, doubling angular resolution in the wave model, and the operational assimilation of QuikSCAT winds. A more detailed account of these changes is presented in Fig. A4 which also shows the history of the first-guess wave height error.

The standard deviation of error in wind speed has reduced over the past 10 years by 40%. As a consequence the contribution of the wind speed error to the wave height error has reduced, so that wave model errors now play a much more prominent role in wave forecasting than in 1995 (Janssen *et al*, 1997). As mentioned in Section 3 we therefore started improving some aspects of the model physics.

Despite the impressive improvements seen in the quality of the forecast wind speed it should be pointed out that there are also problems. The wind speed is biased low with respect to the buoy observations (presently of the order of 25 cm/s) and, associated with the bias problem, there is also a considerable lack of variability in the small scales. The lack of variability is perhaps best illustrated by Fig. 8 which shows a plot of the surface kinetic energy spectrum obtained from QuikSCAT winds and model winds over a three month period. Clearly, the IFS model underestimates variability starting from around total wavenumber 100. The resulting difference in total kinetic energy between observations and model corresponds to a model bias of 10 – 15 cm/s (The remaining part of the wind speed bias stems, according to the QuikSCAT scatterometer, from an underestimation of the energy in the large scales). Note that this lack of variability is reflected in wave model results for the significant wave height. This follows from a comparison of modelled spatial wave height spectra with the ones observed by means of the ENVISAT and Jason altimeters.

In the past there has been extensive discussion in the literature on the shape of the kinetic energy spectrum. From observations and idealized model simulations the consensus nowadays seems to be that beyond the baroclinic instability wavenumber range there are two inertial subranges, an enstrophy cascade for relatively low wave numbers up to a transition wave number  $K_t$  and energy cascade for wavenumbers larger than  $K_t$ . The transition wavenumber is a function of height in such a way that near the surface  $K_t$  is of the order of 100, while in the lower stratosphere  $K_t$  may be as low as 25. The enstrophy cascade corresponds to a  $K^{-3}$  law while the energy cascade has a  $K^{-5/3}$  power law. Most atmospheric models typically miss the energy cascade and therefore lack small scale variability. However, near the surface this problem is less than in the upper layers of the atmosphere.

It has been suggested that the lack of small scale variability is related to the model's inability to represent internal gravity waves. However, even a two level, quasi-geostrophic model can reproduce the observed  $K^{-5/3}$  power law in the mesoscale range convincingly (Tung and Orlando, 2003). Therefore, one would expect that

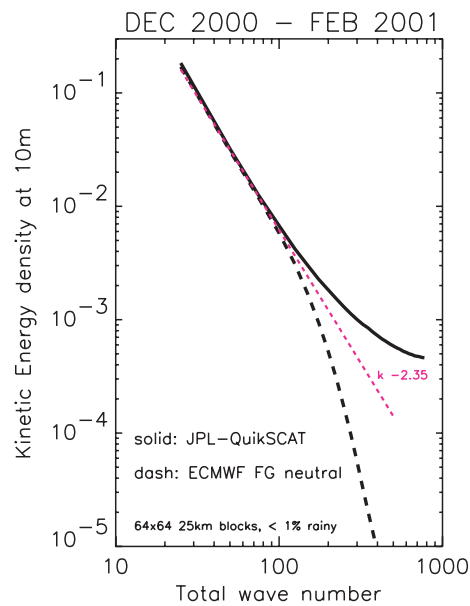


Figure 8: Surface kinetic energy spectrum of QuikSCAT winds and  $T_1$  511 model winds as function of total wave number  $K$  for the period December 2000 until February 2001.

a model such as the IFS should be able to produce an energy cascade in the high wavenumber range. This is clearly not the case, and presumably this is caused by the combination of the interpolations in the semi-Lagrangian scheme and the time-integration scheme which give rise to too much smoothing in the small scales.

Ocean waves are sensitive to the lack of small scale variability since the input source function is proportional to the surface stress. If the lack of variability is related to the numerical treatment of the primitive equations, and it is known that this is a robust property, then there is a simple short term solution available. The lack of small scale variability is accounted for by simply adding 25 cm/s to the windspeed. First experiments with the standalone version of the wave model show very promising results indeed.

## 5 Extreme sea state forecasting

In the early 1960's there was a rapid development of the statistical theory of ocean waves, culminating in the basic evolution equation for the ocean wave spectrum. To lowest order, the probability distribution function (pdf) for the surface elevation was found to be a Gaussian, corresponding to the case of linear waves. It was not realized at that time, however, that dynamical effects of finite amplitude on the pdf can be calculated and result in valuable information on extreme sea states.

Starting point for deriving the energy balance equation for the wave spectrum are a set of deterministic, non-linear evolution equations for the amplitude and phase of the surface gravity waves. Because of nonlinearity, the equation for the second moment (i.e. the wave spectrum) is coupled to the third and fourth moment, and so on. An infinite hierarchy of equations follows and usually this hierarchy is closed by making the statistical assumption that the system remains close to Gaussian. However, finite deviations from the normal distribution are required in order to get a meaningful evolution of the spectrum (due to nonlinear three and four wave interactions). These deviations from Normality can be obtained using a technique originally devised by Chapman and Enskog to calculate the transport properties (such as the molecular viscosity) of fluids. Applied to the appropriate evolution equations for water waves, the result is the well-known Hasselmann equation for four-wave

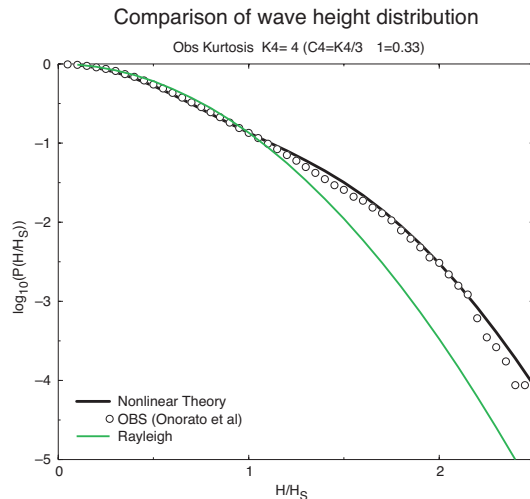


Figure 9: Comparison of theoretical and observed (Onorato *et al*, 2005) wave height distribution. For reference, the linear Rayleigh result is shown as well.

interactions. The deviations from Normality contain, however, useful statistical information in itself, for example one may determine interesting parameters such as the skewness and the kurtosis of the pdf of the surface elevation.

The theoretical approach regarding spectral evolution and the corresponding statistical properties of the sea surface have been validated by Janssen (2003) by means of Monte Carlo simulations of the deterministic evolution equations.

In addition, the theoretical approach compares favourably with wave tank observations by Onorato *et al* (2005). This is shown in Fig. 9 which gives the probability  $P_H(h)$  that instantaneous wave height exceeds  $h$  times the significant wave height  $H_S$ , according to observations, theory (Mori and Janssen, 2005) and according to linear theory (Rayleigh distribution). Note that the theoretical distribution assumes a very simple form, as

$$P_H(h) = e^{-2h^2} [1 + C_4 B_H(h)], \quad B_H(h) = 2h^2 (h^2 - 1). \quad (11)$$

where, with  $\eta$  the surface elevation,  $C_4 = \langle \eta^4 \rangle / (3 \langle \eta^2 \rangle^2) - 1$  is a kurtosis parameter, defined in such a way that it vanishes for a Normal distribution. As can be seen from the Figure and from Eqn. (11), for positive Kurtosis there are considerable increases in the probability of extreme sea states, and, indeed, from the observed time series a number of freak waves were visible.

### 5.1 Operational Implementation

The first consequences of this approach have been implemented already in operations. An essential step in this implementation is a procedure to forecast the kurtosis parameter. Theoretically, the kurtosis is a very complicated expression in terms of the (action) wave spectrum  $N$ . However, for Gaussian-shaped spectra in the narrow band approximation the kurtosis shows a particularly simple dependence on the so-called Benjamin-Feir Index, denoted by  $BFI$ :

$$C_4 = \frac{\pi}{3\sqrt{3}} \times BFI^2,$$

hence the kurtosis depends on the square of the *BFI* (for a detailed derivation see Mori and Janssen, 2005). Here

$$BFI = \varepsilon \sqrt{2} / \sigma'_{\omega},$$

where  $\sigma'_{\omega} = \sigma_{\omega} / \omega_0$  is the relative width of the frequency spectrum,  $\omega_0$  is the angular peak frequency and  $\varepsilon = (k_0^2 \langle \eta^2 \rangle)^{\frac{1}{2}}$  is an integral measure of wave steepness (with  $\langle \eta^2 \rangle$  the average surface elevation variance and  $k_0$  the peak wave number). Therefore, operationally the *BFI* is obtained from the predicted wave spectrum and the kurtosis and other relevant statistical parameters of the sea surface follow then immediately.

It is emphasized that this approach is really an important step forwards. For the past fifty years we have concentrated on the description of the mean sea state. Now, there is perspective to start predicting deviations from the mean sea state, but it is clear that over the oceans still a lot of validation of the skill of the new aspects of the wave forecasting system is required. Validation of the skill of the probabilistic aspects of the wave forecasting system will be pursued in two directions. Using results from the new interim reanalysis we will collocate ship accidents with modelled sea state and kurtosis estimates. This work will be done together with the University of Leuven, Météo-France and the Met Office. The second direction will be an attempt to validate modelled kurtosis with estimates from the radar altimeter. As pointed out in section 3.5, the Radar return signal depends on the surface elevation probability distribution at zero slope and using the known, theoretical shape of the probability distribution function we might be able to estimate parameters such as the kurtosis directly from the wave form (Work together with S. Laxon (UCL) and N. Mori).

## 5.2 Towards a new nonlinear transfer in shallow water

A more intuitively appealing explanation of the formation of freak waves is the following. If waves have a small amplitude then they behave in a linear manner, hence the superposition principle applies. This means that when two wave trains with nearly the same amplitude and wavenumber meet then depending on the phases of the wave trains one finds as extreme twice the amplitude at best (constructive interference). The corresponding pdf of the surface elevation is the Normal distribution and this pdf is regarded as the norm against which to measure extreme events.

Finite amplitude waves are different because due to nonlinearity there are four-wave interactions, hence it is possible to borrow energy and momentum from the neighbouring waves. This is called *nonlinear focussing* and may result in amplification rates of a factor of 5 (rather than the factor of two in linear theory). Therefore, when nonlinear focussing is present extreme events are more likely to occur as is evident from Fig. 9.

It is important to point out that nonlinear focussing and the associated Benjamin-Feir instability is only present in fairly deep water. When water waves approach shallower water (measured by the parameter  $kH$  (with  $k$  wavenumber and  $H$  the water depth)) nonlinearity will give rise to a finite wave-induced stress, resulting in a wave-induced current and deviations from the mean surface elevation. The generation of a current has a damping effect on the Benjamin-Feir instability and, in fact, for  $kH = 1.363$  the Benjamin-Feir instability disappears. In other words, for  $kH < 1.363$  water waves are not subject to nonlinear focussing, and hence it is less likely that freak waves occur in these shallow waters. Because there is a fairly close connection between the Benjamin-Feir instability and the nonlinear transfer in a random sea it follows that at  $kH = 1.363$  the nonlinear transfer should vanish.

In the wave modelling community one is not aware of this particular property of the nonlinear transfer. For  $kH$  of the order 1 the nonlinear transfer is quite active in present day wave models, resulting in considerable downshifts of the wave spectrum. However, according to the present findings, the nonlinear transfer should be quite small, thus there is hardly any downshift. As a consequence the wave spectrum should have a much higher

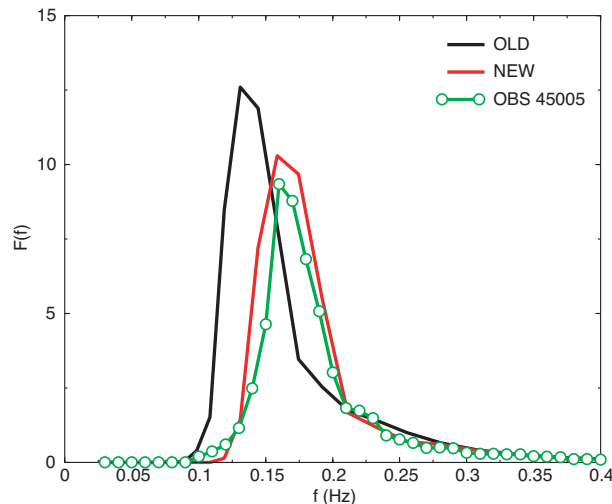


Figure 10: Impact of corrected shallow-water, nonlinear transfer on spectral shape. Observation from Lake Erie at a depth of 14.6 m are shown as well.

peak frequency. Evidence for this is given in Fig. 10, which shows for buoy 45005 (depth is 14.6 m) located in the Western part of Lake Erie a comparison of modelled spectrum of the present version of the wave model and a new version (with corrected nonlinear transfer) with buoy observations. Clearly, the new version has a higher peak frequency and shows close agreement with the observed spectrum. This promising development is now subject to further testing.

## 6 Effects of currents and coastal zone modelling

The WAM model has an option to allow for the effects of ocean currents on wave propagation. Currents may effect ocean waves in the following ways. First, the frequency of the waves gets a Doppler shift, given by the wavenumber times the current velocity. Second, when the current has a horizontal gradient then waves are refracted in a similar way as in the case of depth refraction. However, the most dramatic effects may be found when waves propagate against an ocean current. For sufficiently high current and high frequency, wave propagation is prohibited and wave breaking and wave reflection occurs. The most prominent example of the process of wave blocking is found in the Agulhas current, east of South Africa. The combined effect of current refraction and wave steepening (just prior to wave blocking) is thought to play a role in the formation of freak waves, which occur fairly frequently in the Agulhas current.

We have investigated the impact of currents on the significant wave height field by doing a standalone run with the wave model using monthly mean currents provided by the seasonal forecasting group. Fig. 11 shows the monthly mean difference in wave height field from an experiment with and without currents. All major current systems are visible in this difference plot except perhaps the Gulf stream. However, the amplitude of the differences is fairly small, of the order of 10 cm at best. A comparison with results from Komen *et al* (1994) suggests that in the North Atlantic the modelled current is most likely too weak. Nevertheless, it is expected that in the near future the effects of currents will be included in the seasonal forecasting version of the wave prediction system.

Although on a global scale effects of the current may be fairly modest, it is known that in the coastal zone, in the presence of large tidal currents and surges, currents may modulate wave spectra to a considerable extent.

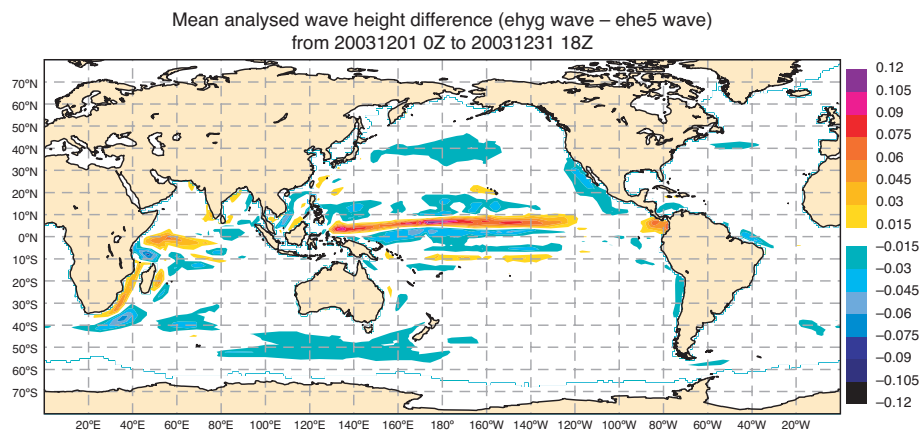


Figure 11: Impact of monthly mean currents from the seasonal forecasting system on the monthly mean significant wave height field. All major current systems are visible in the difference plot except perhaps the Gulf Stream.

A proper modelling of the sea state in the coastal zone, will require therefore the introduction of a coupled storm-surge, ocean wave prediction system. In addition, near the coast additional shallow water effects need to be taken into account. Examples are bottom-induced wave breaking, refraction and perhaps even quasi-resonant three wave interactions. Also, following the work reported in Section 5.2 the shallow water version of the nonlinear four-wave interactions requires attention.

Most of the work (for example the coupling of a storm-surge model and the WAM model), has already taken place during the European Union project Promise. Therefore, a first coastal zone version of the wave forecasting system (presumably replacing the present European Shelf Model) is expected to be ready by 2009, with a more refined system following on in due course.

## 7 Conclusion

At ECMWF there has been a considerable improvement in wave forecasting skill, in particular during the past ten years. Although wave model improvements have contributed to a considerable extent to the improved skill for predicting significant wave height and parameters such as the mean period<sup>1</sup> it is argued in this paper that the major reason of the improvement comes from a higher quality wind field. This conclusion immediately follows from the Figs. 7 and A6. Fig. 7 shows, for given wind fields, the improved skill when improving the wave prediction model. The improvements are fairly modest and last until day 5 of the forecast. By comparing in Fig. A6 scores from the winter of 1997-1998 and from the winter of 2004-2005 it is clear that there are massive improvements to be noted with the recent wave forecasting system, but, evidently, they can only come from an improved quality of forecast wind. Further improvements in wind and wave forecasts are expected from the upcoming high resolution system (T799L91 atmosphere coupled to a 40 km version of the WAM).

Therefore, one may ask the question whether there is any need for wave model improvements. Evidently, there is, at least if one is interested in a realistic representation of the properties of the sea surface. Examples are the coupling of wind and waves which had a beneficial impact on the forecast and the recent improvements seen in the mean frequency of the ocean waves. It is emphasized that forecasting of significant wave height is only

<sup>1</sup>Just recently Fabrice Arhuin from SHOM ran the most recent version of our wave prediction system and WAM cy4 for two winter seasons for the North Atlantic area, using ECMWF wind fields. Compared to buoy data the scatter index for significant wave height reduced from 22% to 13%, a very considerable improvement indeed

one aspect of the wave forecasting problem, the final aim is to obtain a reliable and accurate two-dimensional wave spectrum. This is relevant for many practical applications ranging from ship response studies to sea state effects on altimeter measurements.

Finally, wave model results are sensitive to errors in the forcing wind speed. We have utilized this property of ocean waves to our advantage by using wave model forecast results as a tool to diagnose problems in the atmospheric model (Janssen *et al*, 2000). Examples are the inconsistency between surface wind and stress, the overactivity of the atmospheric forecast, and the lack of small-scale variability. Combined with the two-way interaction of wind and waves this has contributed to maintaining a high quality weather forecasting system.

## A Verification Results

At ECMWF we verify wave forecast and analysis against three types of information. Wave forecast and analysis is validated against independent buoy data for wave height, peak period and mean period. In addition, the spectral shape is validated against frequency spectra. Furthermore, we validate first-guess wave height against altimeter data from ERS-2, ENVISAT and Jason, while first-guess spectra are compared with SAR data. Finally, wave forecasts are validated against the verifying analysis.

The procedures to perform these verifications have been documented and an overview of the skill of the ECMWF wave forecasting system has been presented in Janssen (2004). Here, more recent verifications are briefly discussed.

### A.1 Verification against analysis.

In the Figs. (A1-A3) are shown timeseries of the standard deviation error of forecast wind and ocean wave height against analysis since August 1994 for Northern Hemisphere, Tropics and Southern Hemisphere. In all areas a substantial improvement is noted. In terms of anomaly correlation there is now useful forecast skill in the Tropics up to day 10.

### A.2 Verification of first-guess against altimeter data.

The Figs. (A4-A5) show timeseries of the rms error of first-guess wave height against ERS-2 altimeter wave height and ENVISAT altimeter wave height, respectively. The comparison with ERS-2 data confirms the picture given by the verification against analysis. Note that rms errors against ENVISAT are typically larger than against the ERS-2 data, presumably reflecting the higher variability in the ENVISAT data. Also in Fig. (A5) we have indicated the start of ENVISAT data assimilation with a magenta line and the impact on the assimilation on the quality of the first-guess wave height is clearly visible.

### A.3 Verification of wave model data against Buoy data.

For the Northern Hemisphere winter period we routinely validate forecast wave height and period against buoy data. Fig. A6 shows the progress in forecast skill ECMWF has made in the past 10 years.

The American and Canadian buoy data providers also archive frequency spectra, allowing us to validate spectral shape. Fig. A7 shows the evolution of the equivalent wave height bias as function of wave period from December 2000 and onwards.

Finally, ECMWF is also involved in an intercomparison project with a number of other weather centres, such as UKMO, DWD, NCEP, CMC, Météo-France and FNMOC. A comparison of forecast scores for wind and wave height is given in the Figs. A8 and A9 and it shows that ECMWF clearly leads the other centres.

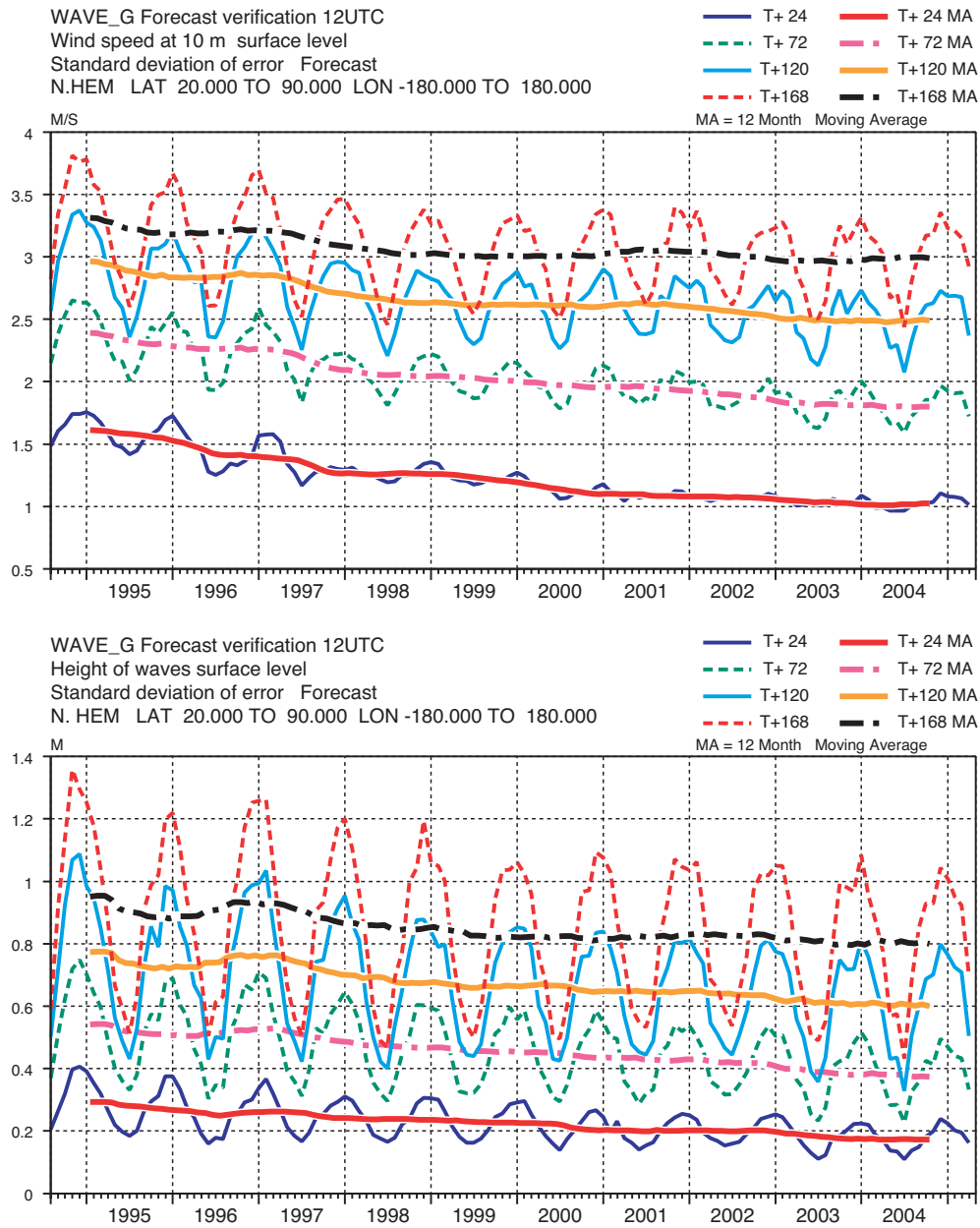


Figure A1: Standard deviation of forecast wind speed and wave height error against analysis for Northern Hemisphere over the period of August 1994 until April 2005. Forecast ranges are T+24, T+72, T+120 and T+168. The 12 month moving average is shown as well.

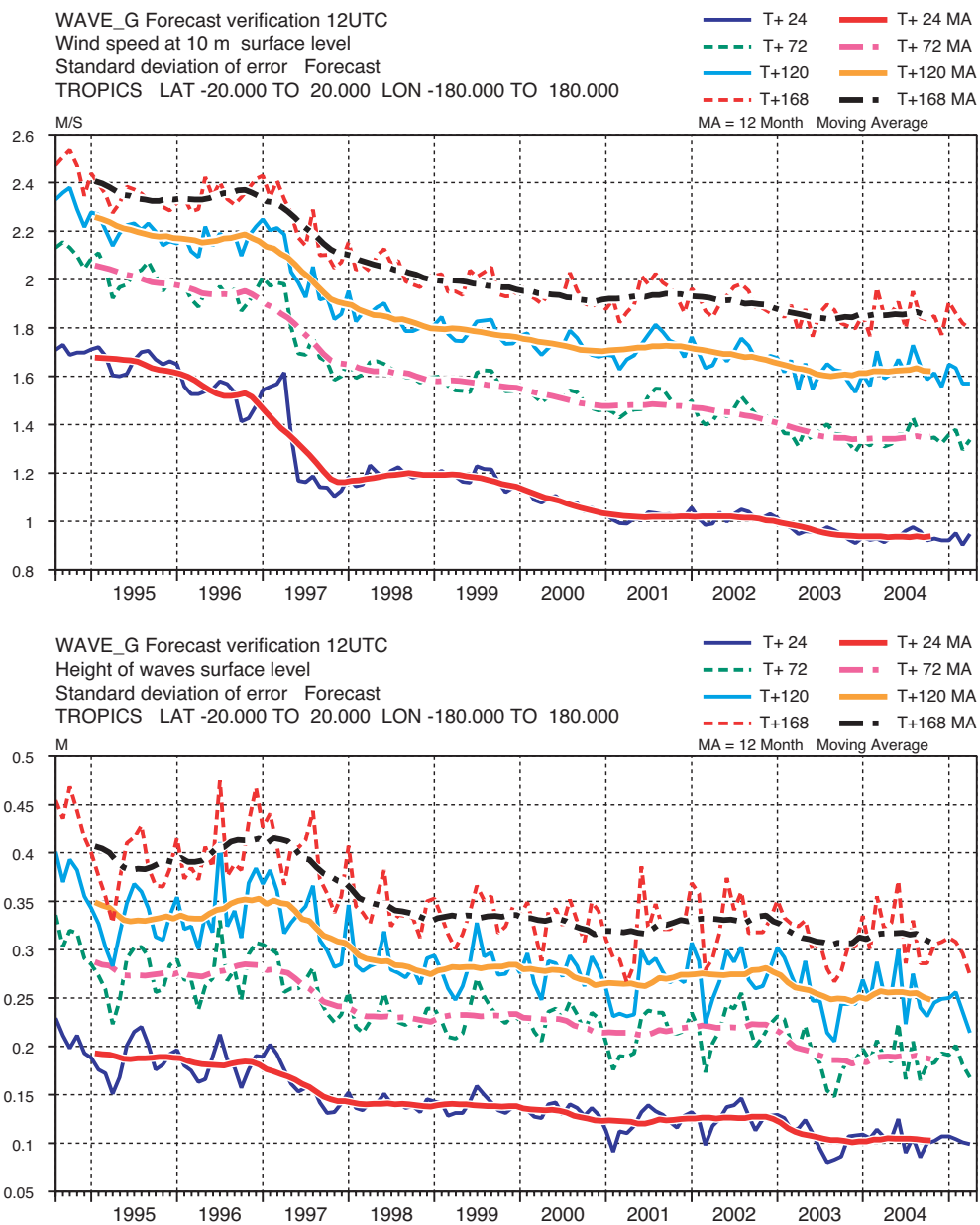


Figure A2: Standard deviation of forecast wind speed and wave height error against analysis for the Tropics over the period of August 1994 until April 2005. Forecast ranges are T+24, T+72, T+120 and T+168. The 12 month moving average is shown as well.

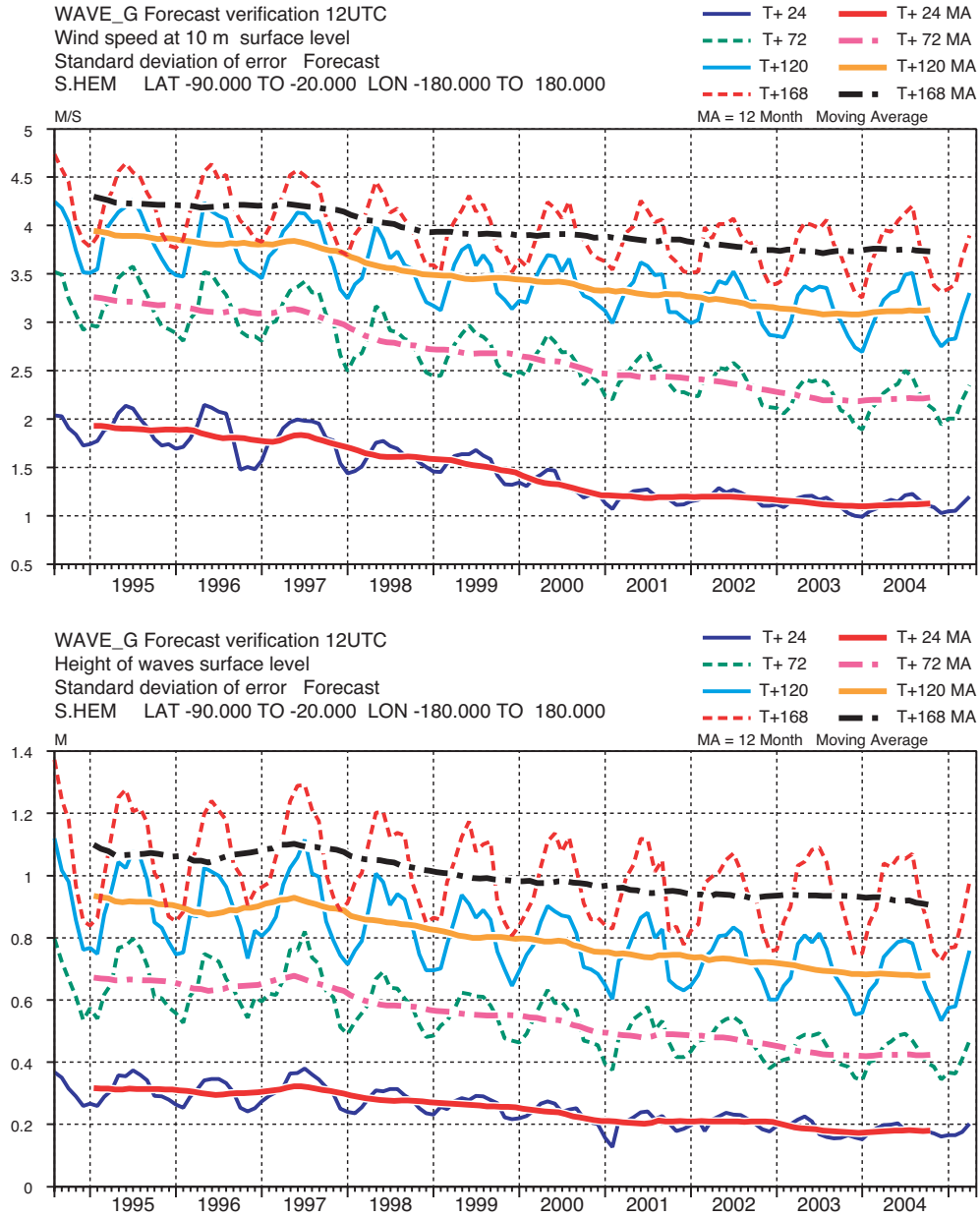


Figure A3: Standard deviation of forecast wind speed and wave height error against analysis for Southern Hemisphere over the period of August 1994 until April 2005. Forecast ranges are T+24, T+72, T+120 and T+168. The 12 month moving average is shown as well.

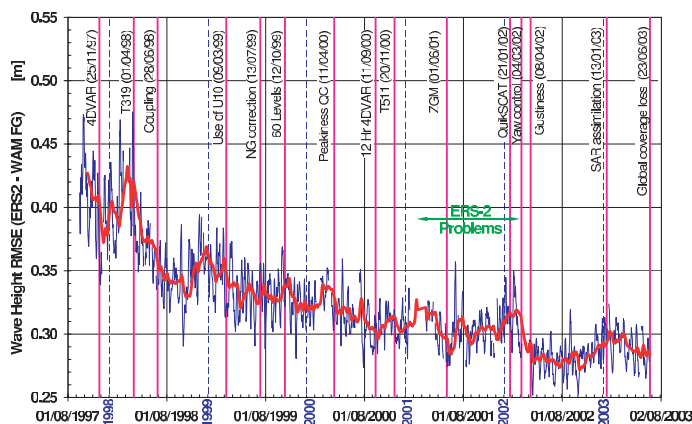


Figure A4: RMS error of first-guess wave height against ERS-2 altimeter data for the whole globe over the period of August 1997 until August 2003. After this date the ERS-2 mission became a local mission, mainly confined to the North Atlantic.

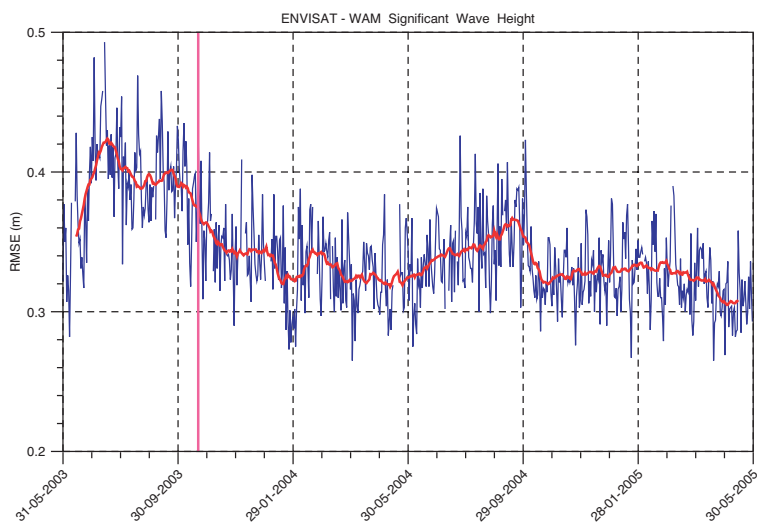


Figure A5: RMS error of first-guess wave height against ENVISAT altimeter wave height for the period of June 2003 until April 2005. The magenta vertical line indicates the time that ECMWF started to assimilate ENVISAT data.

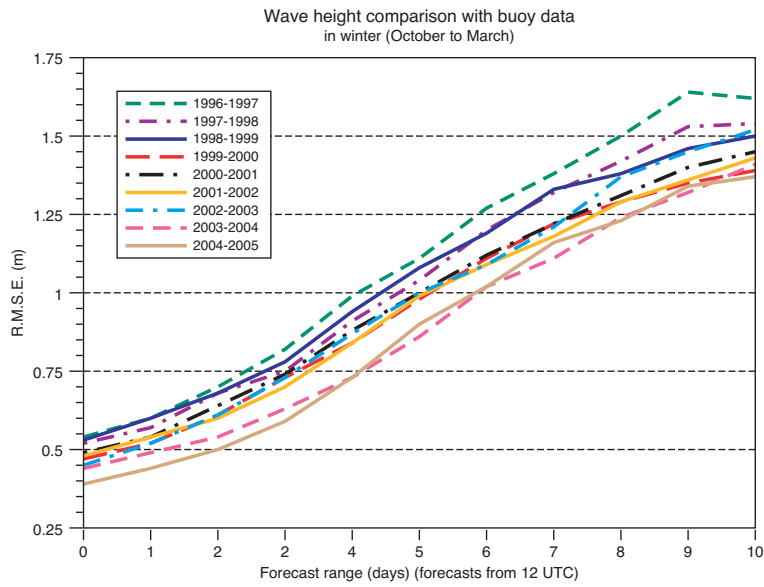


Figure A6: RMS error of analysed and forecast wave height against Buoy wave height data for all winters from 1996 onwards.

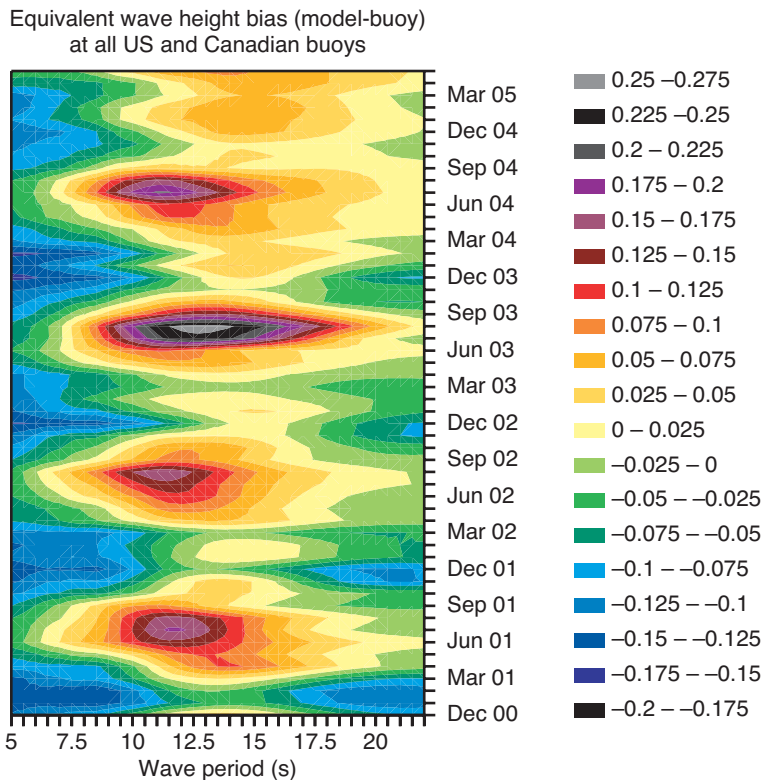


Figure A7: Equivalent wave height bias as function of wave period at all US and Canadian buoy locations for the period December 2000 to May 2005.

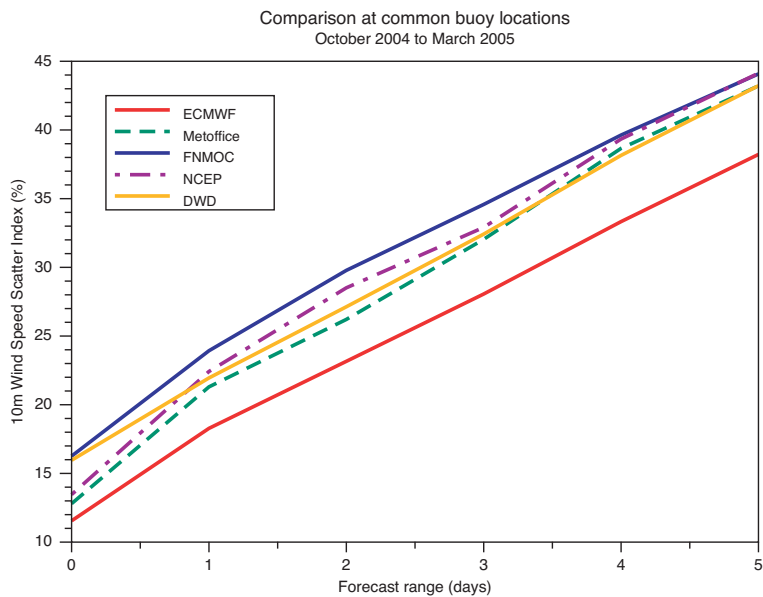


Figure A8: Wind speed scatter index as function of forecast time for different weather centres. Period is winter 2004-2005.

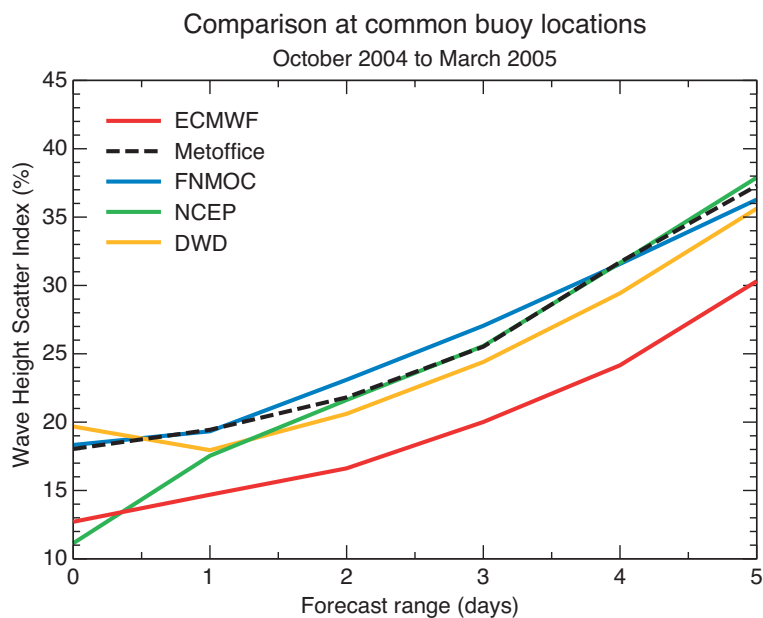


Figure A9: Wave height scatter index as function of forecast time for different weather centres. Period is winter 2004-2005.

## References

- Abdalla, S. and L. Cavaleri, 2002: Effect of wind variability and variable air density on wave modeling. *J. Geophys. Res.* **107**, No. C7,17-1,17-17.
- Bidlot, J.-R., P. Janssen, B. Hansen and H. Günther, 1997. A modified set up of the advection scheme in the ECMWF wave model. *ECMWF Technical Memorandum* **237**.
- Bidlot, Jean-Raymond, Damian J. Holmes, Paul A. Wittmann, Roop Lalbeharry, Hsuan S. Chen, 2002. Inter-comparison of the Performance of Operational Ocean Wave Forecasting Systems with Buoy Data. *Weather and Forecasting* **17**, 287-310.
- Hasselmann, K., 1974. On the spectral dissipation of ocean waves due to whitecapping. *Boundary Layer Meteorol.* **6**, 107-127.
- Hasselmann, S., K. Hasselmann, J.H. Allender and T.P. Barnett, 1985. Computations and parameterizations of the nonlinear energy transfer in a gravity wave spectrum, part 2: Parameterizations of the nonlinear energy transfer for application in wave models. *J. Phys. Oceanogr.* **15**, 1378-1391.
- Hersbach, H. and P.A.E.M. Janssen, 1999. Improvement of the short fetch behavior in the Wave Ocean model (WAM). *J.Atm.Oceanic Technol.* **16**, 884-892.
- Hoffschildt, M., J.-R. Bidlot, B. Hansen and P.A.E.M. Janssen, 1999. Potential benefit of ensemble forecasts for ship routing. *ECMWF Technical Memorandum* **287**.
- Janssen, P.A.E.M., 1989. Wave-induced stress and the drag of air flow over sea waves. *J. Phys. Oceanogr.* **19**, 745-754.
- Janssen, P.A.E.M., 1998. On error growth in wave models. *ECMWF Technical Memorandum* **249**.
- Janssen, P.A.E.M., 2000: ECMWF wave modeling and satellite altimeter wave data, *Satellites, Oceanography and Society*, ed. D. Halpern, Elsevier: Amsterdam. pp. 35-56.
- Janssen, P.A.E.M., 2003. Nonlinear Four-Wave Interactions and Freak Waves. *J. Phys. Oceanogr.* **33**, 863-884.
- Janssen, P.A.E.M., A.C.M. Beljaars, A. Simmons and P. Viterbo, 1992. On the determination of surface stresses in an atmospheric model. *Monthly Weather Review* **120**, 2977-2985.
- Janssen, P.A.E.M., B. Hansen and J.-R. Bidlot, 1997. Verification of the ECMWF Wave Forecasting System against buoy and altimeter data. *Wea. Forecasting*, **12**, 763-784.
- Janssen, P.A.E.M., J. Bidlot, and B. Hansen, 2000. Diagnosis of the ECMWF ocean-wave forecasting system. *ECMWF Technical Memorandum*, **318**.
- Janssen, P.A.E.M., J.D. Doyle, J. Bidlot, B. Hansen, L. Isaksen and P. Viterbo, 2002: Impact and feedback of ocean waves on the atmosphere. in *Advances in Fluid Mechanics*, **33**, Atmosphere-Ocean Interactions, Vol. I, Ed. W.Petrie.
- Janssen, P.A.E.M., 2004. *The Interaction of Ocean Waves and Wind.*, Cambridge University Press, Cambridge, U.K., 300+viii pp.
- Komen, G.J., K. Hasselmann and S. Hasselmann, 1984. On the existence of a fully developed windsea spectrum. *J. Phys. Oceanogr.* **14**, 1271-1285.
- Komen, G.J., L. Cavaleri, M. Donelan, K. Hasselmann, S. Hasselmann, and P.A.E.M. Janssen, 1994: *Dynamics and Modelling of Ocean waves*, Cambridge University Press, Cambridge, U.K., 532 pp.

- Kumar, R., D. Stammer, W.K. Melville, P. Janssen, 2003. Electromagnetic bias estimates based on TOPEX, buoy, and wave model data. *J. Geophys. Research* **108**, 3351, doi:10.1029/2002JC001525.
- Miles, J.W., 1957. On the generation of surface waves by shear flows. *J. Fluid Mech.* **3**, 185-204.
- Mori, N. and P.A.E.M. Janssen, 2005. On Kurtosis and Occurrence Probability of Freak Waves, submitted for publication.
- Onorato, M. R. Osborne, M. Serio and L. Cavaleri, 2005. Modulational Instability and non-Gaussian Statistics in experimental random water-wave trains. *Phys. of Fluids* **17**, 078101.
- Panofsky, H.A., H. Tennekes, D.H. Lenschow and J.C. Wyngaard, 1977. The characteristics of Turbulent velocity components in the surface layer under convective conditions, *Boundary-Layer Meteorology*, **11**, 355-361.
- Saetra, O and Jean-Raymond Bidlot, 2004. Potential Benefits of Using Probabilistic Forecasts for Waves and Marine Winds Based on the ECMWF Ensemble Prediction System. *Weath. Forecasting* **19**, 673-689.
- Saetra, O, Hans Hersbach, Jean-Raymond Bidlot and David S. Richardson, 2004. Effects of Observation Errors on the Statistics for Ensemble Spread and Reliability. *Mon. Weath. Rev.* **132**, 1487-1501.
- Tung, K.K. and W.W. Orlando, 2003. The  $k^{-3}$  and  $k^{-5/3}$  Energy Spectrum of Atmospheric Turbulence: Quasi-geostrophic Two-Level Model Simulation, *J. of Atmos. Sciences*, **60**, 824-835.